Received: 12 December 2016 | Accepted: 27 January 2017

DOI: 10.1111/ijac.12664

ORIGINAL ARTICLE

International Journal of Applied Ceramic TECHNOLOGY

Stabilization of tricalcium phosphate slurries against sedimentation for stereolithographic additive manufacturing and influence on the final mechanical properties

Markus Pfaffinger[1] | **Malte Hartmann**[1] | **Martin Schwentenwein**[2] | **Jürgen Stampfl**[1]

[1]Institute of Material Science and Technology, TU Wien, Vienna, Austria

[2]Lithoz GmbH, Vienna, Austria

Correspondence
Markus Pfaffinger
Email: markus.pfaffinger@tuwien.ac.at

Funding information
TU Wien; Christian Doppler Laboratory

Abstract

Ceramic parts manufactured by lithography-based ceramic manufacturing (LCM) excel in resolution and surface quality. The material for LCM is a photosensitive ceramic particle-filled slurry which needs to have homogeneous properties over time and during each processing step. The goal of this study was to use "mechanical" stabilization for a tricalcium phosphate-filled slurry done by increasing slurry viscosity, solids loading, or inducing thixotropic behavior. The modified slurries were compared with a nonstable reference slurry. While all methods lead to increased storage stability, only the stabilized slurry with 0.5 wt% fumed silica is stable during the printing process.

KEYWORDS

bioceramic, scaffold, stabilization, stereolithography, tricalcium phosphate

1 | INTRODUCTION

In regenerative medicine, tissue engineering (TE) is one of the most attractive field of research and has already been introduced into clinical practice.[1] Among others applications, scaffold based bone repair/regeneration is a main topic. Despite the fact that bone is well known for its self-healing abilities, external interventions are necessary to restore normal function. Beside established treatment methods, like autograft, allograft, or xenograft graftings, biodegradable three-dimensional structures called "scaffold" are used to treat damaged bone.[2,3] Scaffolds can mimic the extra cellular matrix which means providing mechanical support or acting as template for cell attachment. Furthermore, they offer interconnected pore structure and high porosity to allow cell migration, diffusion of nutrients as well as waste products and they can serve as delivery vehicle for drugs.[4,5]

For the fabrication of scaffolds for bone regeneration, various methods are available, like chemical/gas foaming,[6] solvent casting and particulate leaching,[7,8] freeze drying,[9] and thermally induced phase separation[10] or electrospinning.[11] They have in common that pore size, shape, and interconnectivity cannot be fully controlled and are not repeatable. Using additive manufacturing (AM) technologies, structures with tailored porosity and scaffolds for patient specific defects can be manufactured, eg, out of computer tomography (CT) data.[4,12] These layer-by-layer approaches allow the near net-shaped processing of highly complex components.[13] Due to its biocompatibility, osteoconductivity and its chemical and structural similarity to the mineral phase of natural bone, tricalcium phosphate (TCP) is an appealing scaffold material.[3,14]

For AM of TCP scaffolds, direct or indirect techniques are available. Indirect methods use wax or polymer molds produced by AM which are infiltrated with calcium phosphate slurry. After hardening of slurry, the wax or polymer mold is either dissolved or burned out.[12] For direct AM of ceramic parts, selective laser sintering (SLS), fused deposition modeling (FDM), 3D printing, or SLA are used.[12,15-19] The latter uses highly filled suspensions of ceramic particles and photocurable resin. The process is called lithography-based ceramic manufacturing (LCM).[20] By curing the resin with UV- or visible light, the polymer matrix builds up a three-dimensional composite object, called green part.[15] In a consecutive step, the organic binder is removed

in a thermal debinding procedure, which is the most critical manufacturing step. By heating the objects up to 600°C, the polymeric backbone is pyrolized.[21] The residual porous powder compact is then sintered, where consolidation and densification lead to the final ceramic part. The final properties of the ceramic parts strongly depend on the sintering conditions since changes in chemical composition and/or phase composition can occur. The final mechanical performance and biological behavior depends on the microstructural design (grain size and shape, porosity ratio, and pore size) as well as the chemical composition (in grains and grain boundaries).[22]

One main issue in the LCM process is a homogeneous and stable slurry, meaning evenly dispersed ceramic particles in the organic media stabilized against sedimentation, agglomeration, and flocculation during the printing process. The state of the art TCP-filled slurry used at TU Wien is not stable against sedimentation of ceramic powder particles. As a result, over time particles settle to the vat bottom during printing which leads to segregation of slurry in long-lasting (>8 hours) printing processes. This paper deals with different stabilization strategies for a TCP ceramic powder-filled organic-based slurry for LCM. By changing the chemical composition of the slurry, a long-time stable slurry is developed.

Depending on the size of the used powder particles ceramic slurries can be considered as colloidal systems. For the stabilization of colloidal suspensions against sedimentation, aggregation or flocculation steric and electrostatic stabilization or a combination of both, namely electrosteric stabilization are used.[23,24] Additionally, a kind of "mechanical" stabilization can be used which reduces or prevents the thermally induced movement of particles in the organic medium and consequently settling of particles over time. For the latter, three methods are available: using high molecular components, increasing solids loading, or making use of thixotropic behavior. All of those have a change in the rheological behavior of the slurry in common. The developed stabilized slurries were compared with a nonstable reference slurry and processed with the "Blueprinter" machines at TU Wien. These machines are especially developed to process such highly viscous materials. After a thermal debinding step and subsequent sintering step, the mechanical properties of the final TCP parts are tested. Figures 1 and 2 show sintered additive manufactured parts made out of TCP.

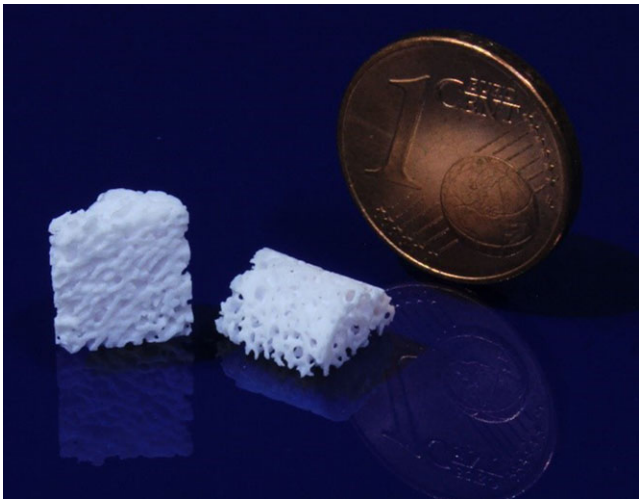

FIGURE 1 Trabecular bone replica made out of tricalcium phosphate (data origin: μ-computer tomography)

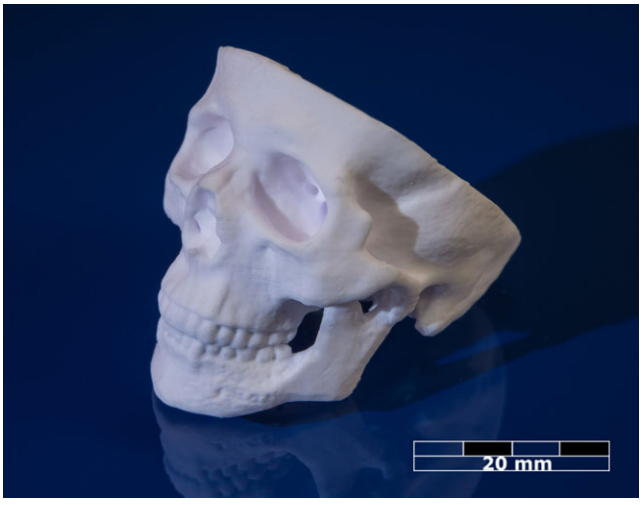

FIGURE 2 Human skull replica made out of tricalcium phosphate (data origin: computer tomography)

2 | EXPERIMENTAL PROCEDURE

2.1 | Ceramic-filled photosensitive slurries

Ceramic-filled slurries for LCM consist of six main constituents: reactive components (commercial (meth-) acrylates), nonreactive organic diluents, photoinitiator, inert light absorber, dispersing agent, and ceramic powder. For the preparation of slurries, all organic components were put in a cup and mixed for 30 minutes on a magnetic stirrer. Afterwards, the TCP powder was added. To homogenize the slurry, a SpeedMixer™ (DAC 150 FVZ; Hauschild, Hamm, Germany) was used for 2 minutes at 3500 rpm.

Table 1 shows the composition of a nonstable reference slurry, indicated as no. (1), as well as the modified slurries no. (2) and no. (3-*x*). In case of slurry no. (2), higher molecular components as well as an increase in the solids loading were used to improve stability of this suspension. Therefore, the acrylate as well as partially the diluent were substituted by a higher viscous alternative. Furthermore, the solids loading of TCP was increased by 4.2 vol%.

TABLE 1 Composition of the tested tricalcium phosphate (TCP) powder-filled slurries

Component (wt%)	Reference Slurry (1)	Slurry (2)	Reference+f-SiO_2 Slurry (3-*x*)
Polyfunctional acrylate (η=90 mPa.s)	8.77		Reference slurry (1) + 0.5-3.0 wt% f-SiO_2
Diacrylate (η=300 mPa.s)		8.47	Reference slurry (1) + 0.5-3.0 wt% f-SiO_2
Dimethacrylate (η=1.28 Pa.s)	7.81	7.56	Reference slurry (1) + 0.5-3.0 wt% f-SiO_2
Solvent	10.50	6.25	Reference slurry (1) + 0.5-3.0 wt% f-SiO_2
Solvent derivative		2.68	Reference slurry (1) + 0.5-3.0 wt% f-SiO_2
Dispersing agent	0.877	0.80	Reference slurry (1) + 0.5-3.0 wt% f-SiO_2
Light absorber	0.003	0.01	Reference slurry (1) + 0.5-3.0 wt% f-SiO_2
Photoinitiator	0.04	0.06	Reference slurry (1) + 0.5-3.0 wt% f-SiO_2
Tricalcium phosphate	72.00	74.17	Reference slurry (1) + 0.5-3.0 wt% f-SiO_2
Solids loading TCP (vol%)	45.5	49.7	45.0-43.0
Solids loading f-SiO_2 (vol%)	–	–	0.22-1.32

Silicon (Si) is essential for bone or connective tissue like cartilage. In literature, references can be found about positive effects of integrated SiO_2 in calcium phosphate ceramics or cements on cell attachment, protein synthesis and resorption of calcium phosphate materials.[25-28] Hence, the stabilization of TCP slurries by adding fumed silica (f-SiO_2) can be a promising alternative. Regarding the organic constituents and the wt% of TCP, the slurries indicated with no. (3-*x*) are identical to the reference slurry no. (1) but additionally 0.5 wt% up to 3.0 wt% of f-SiO_2 were added. Hereby, no. 3-3 refers to 3.0 wt% f-SiO_2, no. 3-2 refers to 2.0 wt% f-SiO_2, no. 3-1 refers to 1.0 wt% f-SiO_2, and no. 3-0.5 refers to 0.5 wt% f-SiO_2. If used, the f-SiO_2 was added last and the slurry was mixed once again for 2 minutes in the SpeedMixer™.

The used TCP powder was a β-TCP powder (Fluka 21218; Sigma Aldrich, St. Louis, MO, USA). It has a D50 value of 2.67 μm. The f-SiO_2 powder with a particle size of 0.007 μm was also from Sigma Aldrich.

2.2 | Evaluation of sedimentation

To evaluate the sedimentation and flocculation of TCP powder, samples of the slurry were filled in test glasses and stored up to 1 week. After defined periods (immediately after mixing, 24, 48 hours and 1 week), the sedimentation was evaluated visually. If sedimentation occurs, the diluent partially separates and floats on top of the samples.

2.3 | Rheology measurement

Additionally to a visual evaluation of the stability of slurries, rheological measurements were conducted. The cone-plate measurements were performed on a rheometer (MC301, Anton Paar, Graz, Austria) with a CP25-1 cone. On the one hand, rotation measurements were used to determine the viscosity in dependence of the shear rate. The shear rate was raised with a constant increase of 1/s up to 100/s followed by a period of 100 s at a constant shear rate of 100/s. For the used Blueprinter machines at TU Wien, the processing limit of ceramic-filled slurries is about 20 Pa.s. In case of printing cellular structures like scaffolds, the maximum viscosity is of about 10 Pa s since the residual uncured slurry after printing needs to be cleaned out of pores.

On the other hand, oscillation measurements were used to evaluate the stability of the slurries as well as their thixotropic behavior. For this purpose, first, an amplitude-sweep was measured (γ=0.01% … 10%, ω=10/s) to identify the viscoelastic region, necessary for the subsequent frequency sweep (γ=0.03 %, ω=0.01 … 100/s). Out of this, the stability of the slurry against sedimentation can be predicted by the relative values of the loss and storage modulus to each other. Finally, a step function of three oscillations (1. γ=0.03%, ω=10/s; 2. γ=10%, ω=62/s; 3. γ=0.03%, ω=10/s) conducted in series was performed to determine the time-dependent build-up and depletion of three-dimensional structure in the slurry. For all rheology measurements, the measuring temperature was 30°C.

2.4 | Additive manufacturing

At TU Wien, bottom-up DLP-based stereolithography machines, called "Blueprinter," are used (Figure 3). They use a custom-made light engine with a LED light source (wavelength of 460 nm) and a digital micromirror device (DMD) selectively projecting light via an optical system onto the bottom of the transparent material vat. Thereby, dynamical masks can be generated. The maximum resolution in *x*/*y*-plane is 25 μm. A special coating system allows the processing of photocurable ceramic-filled slurries with

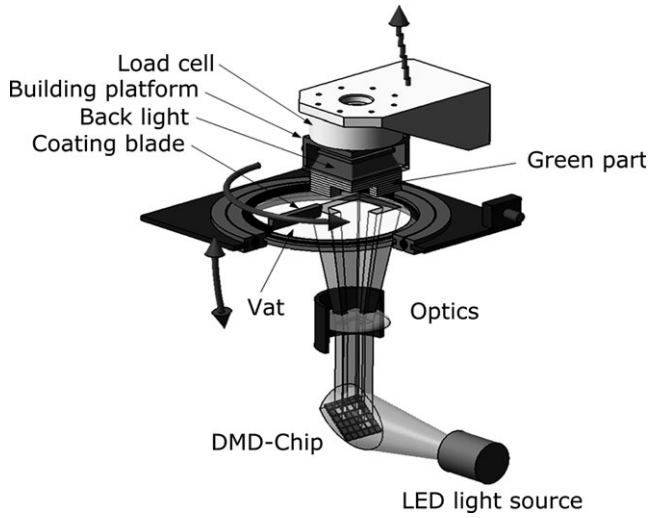

FIGURE 3 Scheme of LCM system at TU Wien (modified[29])

a viscosity of up to 20 Pa.s. The typical layer thickness is between 15 and 100 μm. The size of the building platform is $48\times30\times120$ mm^3.

2.5 | Thermal processing

For the thermal processing, the temperature profile of Figure 4 was used. Thereby, the drying and debinding of the green bodies and the consecutive sintering is executed in one step in a furnace (HTC 08/16; Nabertherm, Lilienthal, Germany) in ambient air. This is necessary to avoid any damage by handling the objects after the debinding process prior to sintering. As sintering substrate, zirconia beads with a mean diameter of 1 mm were used. Sintering atmosphere was air. The temperature profile was taken from Felzmann et al.[29]

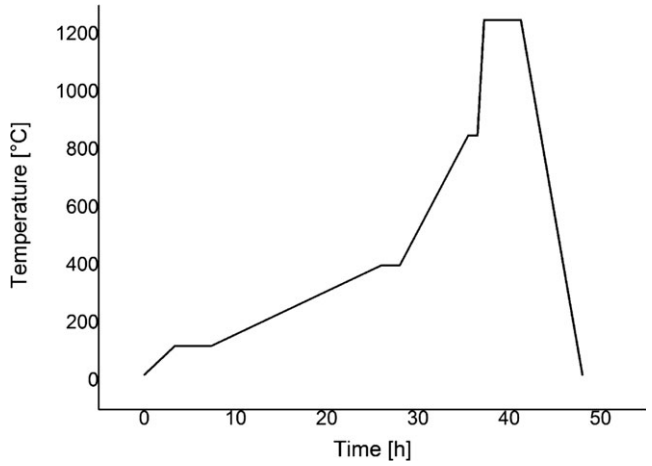

FIGURE 4 Temperature profile for debinding and sintering of tricalcium phosphate green bodies[29]

2.6 | Mechanical properties

To determine the mechanical properties of the sintered parts out of each slurry, 3-point-bending test bars were printed. Two layer orientations (manufacturing direction) with respect to the force impact during testing were analyzed. The designation of layer orientation is according to ISO/ASTM 52921:2013.[30] On the one hand, the orientation of layers is perpendicular to the test direction (orientation YXZ[30]; Figure 5 top). On the other hand, the orientation of layers is in the same direction as the force impact during testing (orientation ZXY[30]; Figure 5 bottom). The specimens were tested "as-fired," without any further surface treatment prior to testing.

The density of the test specimens was measured according to Archimedes' principle to derive the value for the relative density. A value of 3.14 g/cm^3 was used as theoretical density of TCP ceramics.

Furthermore, SEM analysis of sintered and fractured specimens (fracture surface perpendicular to layer orientation) as well as analysis of ground and polished cross-sections of sintered parts were made.

3 | RESULTS AND DISCUSSION

3.1 | Long-time stability of slurry

The application of higher molecular constituents compared to the reference slurry no. (1) as well as the addition of f-SiO_2 leads to an increase in slurry viscosity (Figure 6). Since the processing limit of slurries for the used "Blueprinter" machines is 20 Pa.s, slurries with f-SiO_2 weight fraction of 1 wt% and higher (slurry no. (3-1), (3-2), and (3-3)) cannot be used. Slurry no. (2) and (3-0.5) satisfy the requirements. They are also suitable for the production of porous geometries (max. viscosity of about 10 Pa.s).

Figure 7 shows samples of slurry formulations no. (1), (2), and (3-0.5) immediately after mixing, after 24 and 48 hours as well as after 1 week. The reference slurry shows strong sedimentation over time; further, the diluent floats to the surface. Slurry (2) and (3-0.5) show stability over at least 1 week of storage which is sufficient for

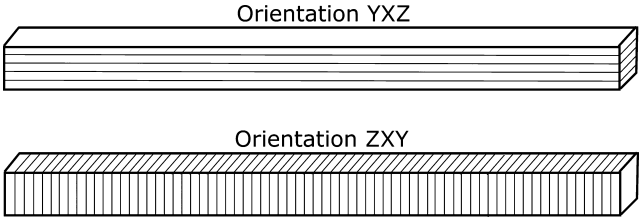

FIGURE 5 Two different layer orientations in 3-point-bending test specimens according to ISO/ASTM 52921:2013[30]

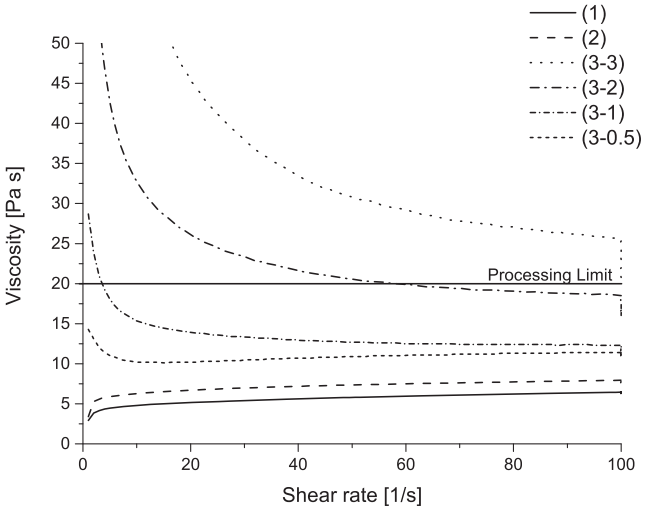

FIGURE 6 Rotation rheology measurement of viscosity of slurries no. (1), (2), (3-1), (3-2), (3-3), and (3-0.5) in dependence of shear rate (processing limit of 20 Pa.s for slurries at Blueprinter machines)

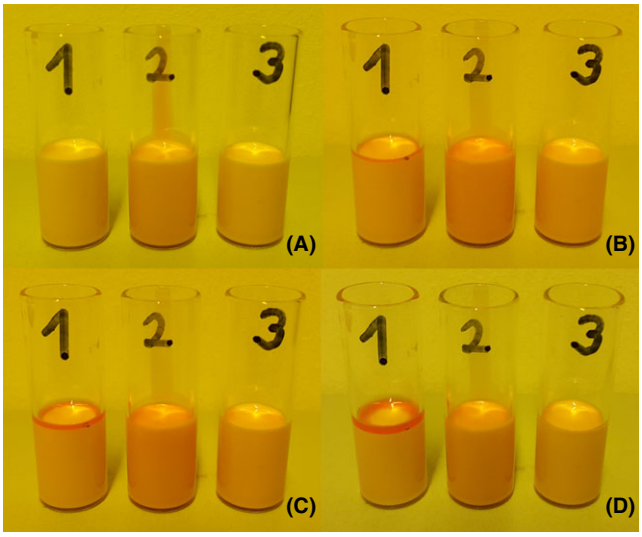

FIGURE 7 Evaluation of long-time stability of slurries no. (1), (2) and (3-0.5) after (A) mixing, (B) 24 h, (C) 48 h, (D) 1 wk

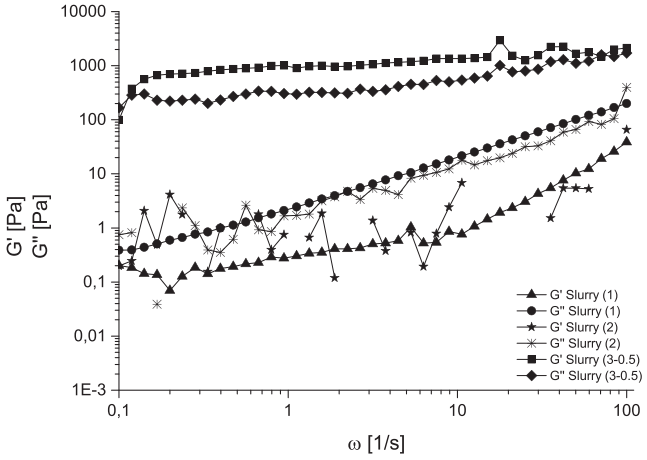

FIGURE 8 Frequency sweep rheology measurement of storage modulus (G′) and loss modulus (G″) of tricalcium phosphate slurries (no. (1), (2), and (3-0.5)) measured at 30°C

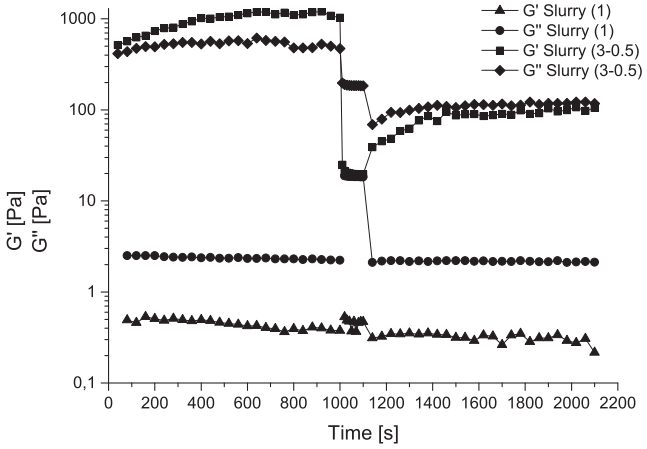

FIGURE 9 Oscillation rheology measurement (three oscillation in series 1. γ=0.03%, ω=10 rad/s; 2. γ=10%, ω=62 rad/s; and 3. γ=0.03%, ω=10 rad/s) of tricalcium phosphate slurries no. (1) and (3-0.5) measured at 30°C

additive manufacturing processes. No sedimentation of ceramic particles or floating of diluent could be observed. Out of a frequency sweep rheology measurement through the relative values of G′ and G″ to each other, the stability of the ceramic slurries can be evaluated. As Figure 8 shows, for slurry no. (1) and (2), G″ is larger than G′ independent of the deformation frequency meaning viscous behavior dominates. Hence, these slurries are not stable against sedimentation.

In contrast, for slurry no. (3-0.5), elastic behavior dominates meaning that stabilization of slurry with f-SiO_2 works the intended way. The resulting three-dimensional network of hydrogen bonds in the slurry prevents sedimentation of TCP particles. For ω>0.12/s, the value for G′ is higher than G″. As a consequence, no sedimentation will occur during printing as slurry is moved while coating. However, long-time stability during storage of slurry cannot be expected since for ω<0.12/s the value for G″ is higher than G′.

The results of the step function oscillation measurement in Figure 9 show no thixotropic behavior for reference slurry no. (1). Slurry no. (3-0.5), however, shows a time-dependent structure build-up. After the depletion of structure in the slurry and consequently viscous behavior during the second oscillation step, relaxation of the slurry starts with beginning of the oscillation step 3. Thixotropic behavior can be supposed. The measuring time of step 3 of 1000 seconds was not long enough to obtain full relaxation. The relaxation time for the intersection of G′ and G″ was calculated as 30.66 minutes.

TABLE 2 Results for mechanical properties from 3-point-bending tests of sintered specimens manufactured out of slurry (1), (2) as well as (3-0.5)

Mechanical properties	Sintered parts out of					
	Slurry (1) n=15		Slurry (2) n=24		Slurry (3-0.5) n=21	
	YXZ	ZXY	YXZ	ZXY	YXZ	ZXY
σ_B (MPa)	19.60±1.9	21.07±1.9	14.70±1.1	6.98±1.4	12.86±0.8	12.15±0.7
σ_0 (MPa)	22.19	21.64	15.20	7.54	13.21	12.47
m	9.52	12.45	15.48	5.77	19.15	20.45
ρ (% theor. ρ)	87.99±1.70		82.80±0.48		89.10±0.59	
Porosity (%)	12		17.2		10.9	

n, number of samples; σ_B, bending strength; σ_0, Weibull strength; *m*, Weibull modulus.

3.2 | Mechanical Properties

For mechanical analysis tests, specimens were manufactured out of slurry no. (1), (2), and (3-0.5). The used exposure energy for layer thickness of 25 μm was 360 mJ/cm². The 3-point-bending specimens were manufactured in two different directions to obtain the information of the resulting mechanical properties as well as the information about the influence of layer adhesion. Table 2 shows the bending strength σ_B of specimens manufactured out of slurries no. (1), (2) and (3-0.5) in respect of their layer orientation. A Weibull statistic was made (*m*=Weibull modulus, σ_0=Weibull strength). Furthermore, the relative density was measured for each type. Regarding specimens made out of slurry no. (1) isotropic mechanical properties can be accepted. The layer orientation does not influence the bending strength, meaning inside one layer as well as at layer borders the objects have the same structural composition. In contrast, specimens made out of slurry no. (2) have lower bending strength. This is caused by the lower relative density. Moreover, they show a strongly anisotropic behavior. The higher molecular polyethylene glycol derivative

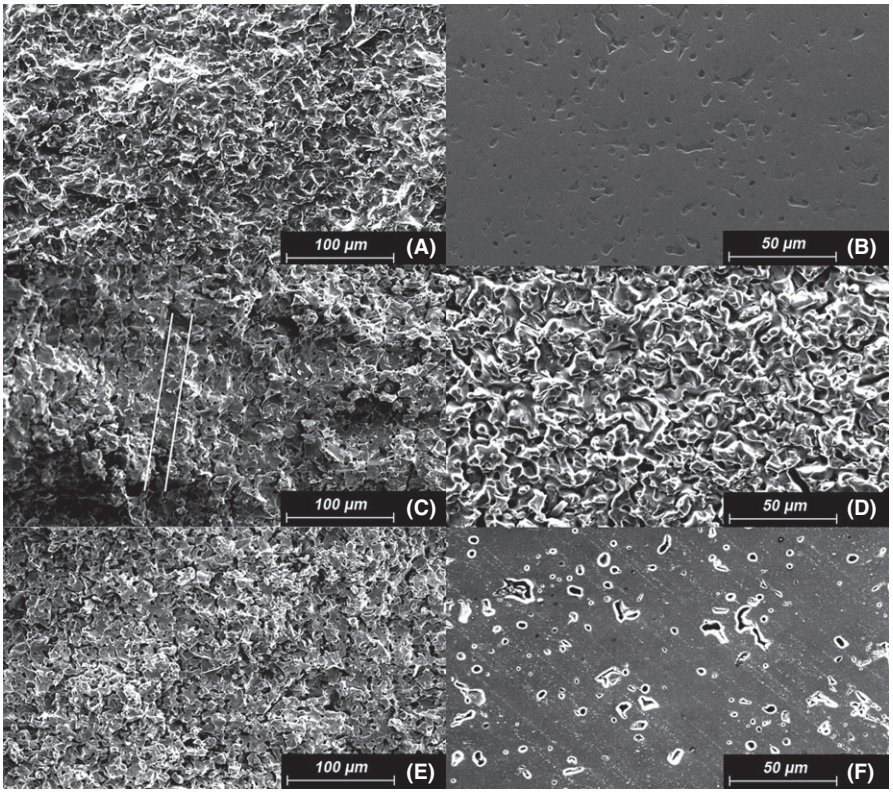

FIGURE 10 Left row: SEM images of fracture surfaces of sintered specimens (perpendicular to layer orientation) right row: polished surfaces of sintered specimens (along one layer) (A), (B) specimens out of slurry no. (1), (C), (D) specimens out of slurry no. (2), (E), (F) specimens out of slurry no. (3-0.5)

affects the polymerization of one layer. Caused by the reduced compatibility between reactive monomers and non-reactive diluent separation occurs during the polymerization, resulting in inhomogeneous properties inside one layer. This weakens the adhesion between layers (see Figure 10), consequently leading to lower bending strength for samples where force vector of impact is in direction of layer borders orientation. Regarding specimens made out of slurry no. (3-0.5), there is almost no difference in bending strength depending on the layer orientation. This means, like for slurry no. (1), there is constant structural composition in every region of green bodies. However, the addition of f-SiO_2 leads to a drop in bending strength compared to slurry no. (1) without f-SiO_2. Si stabilizes the α-phase of TCP.[31] Out of the density difference between β- and α-TCP resulting stress conditions lead to reduced bending strength.

3.3 | Microstructure and fracture surfaces

The fracture surfaces of the tested 3-point-bending specimens were analyzed in a SEM. Furthermore, ground and polished surfaces of specimens were analyzed. Figure 10A shows a homogeneous microstructure for specimens out of slurry no. (1), no layer information can be observed. Same holds for the polished surface (Figure 10B). In contrast Figure 10C shows for specimens out of slurry no. (2) numerous pores aligned at layer borders (white markings). This is because of inhomogeneous layers and consequently insufficient layer adhesion. The fracture orientation for those parts is mostly in direction of layer borders. Figure 10D shows a more porous microstructure for specimens made out of slurry no. (2) resulting in lower density and consequently lower bending strength. Regarding Figure 10E a fracture surface of a specimen out of slurry no. (3-0.5) no layer orientation can be observed. Hence, the bending strength of these specimens is isotropic. No influence of layer orientation with respect to the force vector during testing is evident. The corresponding image of a ground surface (Figure 10F) shows a homogeneous microstructure with macro pores. Those specimens out of slurry no. (3-0.5) feature the highest densities of all samples (89.1% theoretical ρ). However, the integration of f-SiO_2 leads to a decrease in bending strength.

4 | CONCLUSION

The goal of this study was the development of a TCP slurry stable against sedimentation during LCM process. The presented AM technology offers the possibility of manufacturing ceramic parts which excel in high resolution and surface quality. Using TCP as a degradable bioceramic material, bioinspired or biomimetic parts like bone scaffolds or bone prostheses can be produced. One main issue for LCM is a photosensitive ceramic-filled slurry stable against sedimentation, aggregation, and flocculation of ceramic particles during the printing process to obtain ceramic parts with homogeneous and isotropic mechanical properties. An increase in slurry viscosity using higher molecular alternatives for monomers and diluents as well as an increase in solids loading do not lead to a more stable slurry during printing but both methods lead to a significant increase in storage stability. It could be shown that by adding f-SiO_2 thixotropic behavior can be incorporated to an originally nonstable TCP slurry, thus stabilizing it against sedimentation at a slurry viscosity of about 10 Pa.s. Therefore, the flawless production of objects with long-lasting production times (>8 hours) can be guaranteed. Furthermore, the consecutive manufacturing of parts without changing slurry or reconditioning and homogenization in between subsequent printing processes is possible.

The integration of f-SiO_2 in TCP slurries, however, leads to a drop in mechanical properties of the manufactured objects. The beneficial effect of SiO_2 on cell attachment and cell proliferation at additively manufactured TCP bone scaffolds as well as its effect on degradation behavior and time have to be evaluated in future.

ACKNOWLEDGMENTS

The research presented in this paper was conducted at the TU Wien. We gratefully acknowledge the financial support from the Christian Doppler Laboratory for Photopolymers in Digital and Restorative Dentistry.

REFERENCES

1. Meyer U, Wiesmann H-P. Tissue engineering: a challenge of today's medicine. *Head Face Med*. 2005;1:2.
2. Hutmacher DW, Schantz JT, Lam CXF, Tan KC, Lim TC. State of the art and future directions of scaffold-based bone engineering from a biomaterials perspective. *J Tissue Eng Regen Med*. 2007;1:245-260.
3. O'Brien FJ. Biomaterials & scaffolds for tissue engineering. *Mater Today*. 2011;14:88-95.
4. Bose S, Vahabzadeh S, Bandyopadhyay A. Bone tissue engineering using 3D printing. *Mater Today*. 2013;16:496-504.
5. Mouriño V, Boccaccini AR. Bone tissue engineering therapeutics: controlled drug delivery in three-dimensional scaffolds. *J R Soc Interface*. 2010;7:209-227.
6. Harris LD, Kim BS, Mooney DJ. Open pore biodegradable matrices formed with gas foaming. *J Biomed Mater Res*. 1998;42:396-402.
7. Sin D, Miao X, Liu G, et al. Polyurethane (PU) scaffolds prepared by solvent casting/particulate leaching (SCPL) combined with centrifugation. *Mater Sci Eng, C*. 2010;30:78-85.
8. Wake MC, Gupta PK, Mikos AG. Fabrication of pliable biodegradable polymer foams to engineer soft tissues. *Cell Transplant*. 1996;5:465-473.

9. Haugh MG, Murphy CM, O'Brien FJ. Novel freeze-drying methods to produce a range of collagen-glycosaminoglycan scaffolds with tailored mean pore sizes. *Tissue Eng Part C Methods*. 2010;16:887-894.
10. Pavia FC, La Carrubba V, Piccarolo S, Brucato V. Polymeric scaffolds prepared via thermally induced phase separation: tuning of structure and morphology. *J Biomed Mater Res A*. 2008;86:459-466.
11. Lannutti J, Reneker D, Ma T, Tomasko D, Farson D. Electrospinning for tissue engineering scaffolds. *Mater Sci Eng, C*. 2007;27:504-509.
12. Vorndran E, Klarner M, Klammert U, et al. 3D Powder printing of β-tricalcium phosphate ceramics using different strategies. *Adv Eng Mater*. 2008;10:B67-B71.
13. Wohlers Associates Ed. Wohlers Report 2016. Fort Collins, Colorado; 2016.
14. Li X, Li D, Lu B, Wang L, Wang Z. Fabrication and evaluation of calcium phosphate cement scaffold with controlled internal channel architecture and complex shape'. *Proc Inst Mech Eng [H]*. 2007;221:951-958.
15. Griffith ML, Halloran JW. Freeform fabrication of ceramics via stereolithography. *J Am Ceram Soc*. 1996;79:2601-2608.
16. Chartier T, Chaput C, Doreau F, Loiseau M. Stereolithography of structural complex ceramic parts. *J Mater Sci*. 2002;37:3141-3147.
17. Kim K, Yeatts A, Dean D, Fisher JP. Stereolithographic bone scaffold design parameters: osteogenic differentiation and signal expression. *Tissue Eng Part B Rev*. 2010;16:523-539.
18. Safronova TV, Putlayev VI, Evdokimov PV, et al. *Black Powders of Calcium Phosphates for Stereolithography*, presented at the Сборник трудов XIII Российско-Китайского Симпозиума «Новые материалы и технологии» (AMP-2015), 21-25 сентября 2015, ISBN 978-5-902063-53-7. Vol 2. 2015:604.
19. Bian W, Li D, Lian Q, et al. Fabrication of a bio-inspired beta-Tricalcium phosphate/collagen scaffold based on ceramic stereolithography and gel casting for osteochondral tissue engineering. *Rapid Prototyp J*. 2012;18:68-80.
20. Schwentenwein M, Schneider P, Homa J. Lithography-based ceramic manufacturing: a novel technique for additive manufacturing of high-performance ceramics. *Adv Sci Technol*. 2014;88:60-64.
21. Bae C-J, Halloran JW. Influence of residual monomer on cracking in ceramics fabricated by stereolithography. *Int J Appl Ceram Technol*. 2011;8:1289-1295.
22. Champion E. Sintering of calcium phosphate bioceramics. *Acta Biomater*. 2013;9:5855-5875.
23. Horn RG. Surface forces and their action in ceramic materials. *J Am Ceram Soc*. 1990;73:1117-1135.
24. Lewis JA. Colloidal processing of ceramics. *J Am Ceram Soc*. 2000;83:2341-2359.
25. Ning CQ, Mehta J, El-Ghannam A. Effects of silica on the bioactivity of calcium phosphate composites in vitro. *J Mater Sci Mater Med*. 2005;16:355-360.
26. Langstaff S, Sayer M, Smith TJN, Pugh SM, Hesp SAM, Thompson WT. Resorbable bioceramics based on stabilized calcium phosphates. Part I: rational design, sample preparation and material characterization. *Biomaterials*. 1999;20:1727-1741.
27. Langstaff S, Sayer M, Smith TJN, Pugh SM. Resorbable bioceramics based on stabilized calcium phosphates. Part II: evaluation of biological response. *Biomaterials*. 2001;22:135-150.
28. Pietak AM, Reid JW, Stott MJ, Sayer M. Silicon substitution in the calcium phosphate bioceramics. *Biomaterials*. 2007;28:4023-4032.
29. Felzmann R, Gruber S, Mitteramskogler G, et al. Lithography-based additive manufacturing of cellular ceramic structures. *Adv Eng Mater*. 2012;14:1052-1058.
30. I. ISO/ATM, 'ISO/ASTM 52921. 2013 - Standard terminology for additive manufacturing - coordinate systems and test methodologies'. 2013.
31. Mestres G, Le Van C, Gineba MP. Silicon-stabilized α-tricalcium phosphate and its use in a calcium phosphate cement. Characterization and cell response. *Acta Biomater*. 2012;8:1169-1179.

How to cite this article: Pfaffinger M, Hartmann M, Schwentenwein M, Stampfl J. Stabilization of tricalcium phosphate slurries against sedimentation for stereolithographic additive manufacturing and influence on the final mechanical properties. *Int J Appl Ceram Technol*. 2017;00:1-8.